

## High-Resolution Solid-State $^{13}\text{C}$ NMR Study of Poly(vinyl isobutyl ether) / Poly( $\epsilon$ -L-lysine) Blends

Atsushi Asano<sup>\*</sup>, Yoshifumi Murata, Takuzo Kurotsu

*Department of Applied Chemistry, National Defense Academy, Japan*

*Hashirimizu 1-10-20, Yokosuka, Kanagawa 239-8686, Japan*

*E-mail : asanoa@nda.ac.jp*

### Abstract

Several kinds of polymer blends of Poly(vinyl isobutyl ether) (PVIBE) and Poly( $\epsilon$ -L-lysine) ( $\epsilon$ -PL) were prepared by solvent-cast method from chloroform/methanol=9/1 solution.  $^1\text{H}$  spin-lattice relaxation curves for both PVIBE and  $\epsilon$ -PL, which are indirectly obtained from well-resolved  $^{13}\text{C}$  cross-polarization with magic-angle-spinning NMR (nuclear magnetic resonance) spectra, suggest that the blends are partially miscible on a 100 nm scale range and the miscibility depends on the composition. A two-spin model was used to simulate the relaxation curves taking into account the contribution of a  $^1\text{H}$  spin-diffusion rate between the two spins. Furthermore, it is found that the mixing  $\epsilon$ -PL to PVIBE is largely influenced the crystallinity of PVIBE but that of  $\epsilon$ -PL is little affected.

### Introduction

A thermoplastic or an elastic polymer is used widely for engineering purposes. To improve physical or chemical properties of polymers for some purposes, we often made use of mixing another polymer to these kinds of engineering polymers. Therefore, instead of synthesizing a brand-new polymer with all the properties we want, we try to mix two polymers together to form a blend that we hopefully have some properties of both. Recently, with a raise of public awareness to ecology, engineering polymers are tend to be required to have properties of eco-friendliness, especially when out of use.

Poly( $\epsilon$ -L-lysine) ( $\epsilon$ -PL) has attracted an attention as a novel biodegradable material [1-3].  $\epsilon$ -PL is microbially produced, safe for human beings, a water-soluble semicrystalline polymer, and has an antibacterial activity. Some kinds of foods contain it as preservatives. Since the  $\epsilon$ -PL has a good biodegradable/biocompatible property,  $\epsilon$ -PL can be used as a new environmental-compatible polymer.  $\epsilon$ -PL is, however, too brittle and low degree of polymerization to use engineering purposes as it is, so that it may be used as an additive for a synthetic polymer to give biodegradability or antibacterial activity.

Poly(vinyl isobutyl ether) (PVIBE) is a thermoplastic, elastic, and semicrystalline polymer, and used as a plasticizer. The blending of PVIBE and  $\epsilon$ -PL makes it possible to become a new biodegradable material or plasticizer. Furthermore, the blend consists of semicrystalline/semicrystalline polymers. It is interesting to study the morphology of such a semicrystalline polymer blend, because both crystallinity and miscibility largely influence a mechanical property of a polymer blend.

In this study, we study the relationship between the crystallinity and the miscibility of the semicrystalline polymer blend, PVIBE/ $\epsilon$ -PL, by solid-state  $^{13}\text{C}$  NMR technique. The crystallinity is estimated from a solid-state  $^{13}\text{C}$  NMR spectra obtained with cross-polarization and magic-angle-spinning (CPMAS) technique. The miscibility is discussed from the  $^1\text{H}$  spin-lattice relaxation curves indirectly obtained from the  $^{13}\text{C}$  CPMAS NMR spectra.

### Experimental

**Sample Preparation.**  $\epsilon$ -PL (repeating unit RU is  $-\text{NHCH}_2\text{CH}_2\text{CH}_2\text{CH}_2\text{CH}(\text{NH})\text{CO}-$ , relative weight-average molecular weight  $M_w$  is about a few 1,000, the glass-transition temperature  $T_g$  is ca. 323 K, and the melting point  $T_m$  is ca. 443 K) was provided from Chisso Corporation as a solid powder. PVIBE (RU is  $-\text{CH}_2\text{CH}(\text{OCH}_2\text{CH}(\text{CH}_3)_2)-$ ,  $M_w$  600,000,  $T_g$  ca. 253 K, and  $T_m$  ca. 328 K) was obtained from Scientific Polymer Products, Inc. They were used without further purification. PVIBE and  $\epsilon$ -PL were dissolved in chloroform/methanol=9/1 volume ratio at a concentration of about 15 w/v% and mixed at weight ratios of 10/1, 10/2, 10/3, 10/4, and 10/5. The opaque and elastic films of PVIBE/ $\epsilon$ -PL blends were obtained from casting the respective chloroform/methanol=9/1 solutions on a Teflon plate at 40°C and further dried under vacuum at 40°C for 1 or 2 days.

**NMR Measurements.**  $^{13}\text{C}$  NMR measurements were made using a Bruker DMX500 spectrometer operating at 125.76 MHz for  $^{13}\text{C}$  and 500.13 MHz for  $^1\text{H}$ . High-resolution solid-state  $^{13}\text{C}$  NMR spectra were obtained by the combined use of cross polarization (CP) and magic-angle spinning (MAS) with  $^1\text{H}$  high-power dipolar decoupling. The radio-frequency field strengths for  $^1\text{H}$  was 55.6 kHz and for  $^{13}\text{C}$  50.0 kHz. The  $^1\text{H}$  decoupling frequency was chosen to be 3 ppm down-field from tetramethylsilane (TMS) and the two-pulse-phase-modulation decoupling method [4] is used. The MAS frequency is chosen to obtain a clear spectrum at the aliphatic region without overlapping of the artificial spinning side bands of the CO carbons. The MAS frequency of 10 kHz did not show the side bands on the peaks at the aliphatic region. At such a much higher speed, the efficiency of CP enhancement between  $^1\text{H}$  and  $^{13}\text{C}$  nuclei was steeply getting worse. In order to overcome the decreased CP efficiency, the ramped-amplitude CP method was used [5, 6].  $^{13}\text{C}$  chemical shifts were measured relative to TMS using the methine carbon signal at 29.48 ppm for solid adamantane as an external standard. The  $^1\text{H}$  spin-lattice relaxation time in the laboratory frame ( $T_1^{\text{H}}$ ) was indirectly measured from well-resolved  $^{13}\text{C}$  signals enhanced by CP of 800 $\mu\text{s}$  applied after the  $^1\text{H}$   $\pi$  pulse.

### Results and Discussion

**Crystallinity.** Figure 1 shows the observed  $^{13}\text{C}$  CPMAS NMR spectra of pure PVIBE, pure  $\epsilon$ -PL, and the PVIBE/ $\epsilon$ -PL blends at weight fractions of 10/1, 10/3, and 10/5. The peak assignments are also written in the figure. The real contents of PVIBE/ $\epsilon$ -PL blends were ascertained by  $^1\text{H}$  dipolar-decoupling (DD) with MAS spectra, because the peak intensity in the  $^{13}\text{C}$  CPMAS NMR spectra is distorted by the difference in the efficiency of  $^1\text{H}$ - $^{13}\text{C}$  CP enhancement, which depends on a molecular motion; each residue has a characteristic molecular motion. The DDMAS  $^{13}\text{C}$  NMR spectrum gives the correct unit-mole ratio of PVIBE/ $\epsilon$ -PL. The converted weight ratios from the observed mole ratio were equal to the mixing weight ratio of 10/1 to 10/5 within an error of 5% (not shown). The  $^{13}\text{C}$  spectrum of  $\epsilon$ -PL is similar to the previously observed one in ref [2]. The doublet of

carbonyl peaks at 178.5 and 177.0 ppm are observed more clearly in the current solid-state  $^{13}\text{C}$  CPMAS NMR spectrum. There are also small differences in the chemical shifts between the previous and the current spectrum. These may be due to a difference of sample preparation. The current  $\epsilon$ -PL is cast from a methanol solution, while the previous  $\epsilon$ -PL is from a water solution.

Similarly, the  $^{13}\text{C}$  NMR spectrum of PVIBE is affected by the content of methanol; methanol is a poor solvent for PVIBE. The crystallinity is largely influenced by the amount of methanol. For

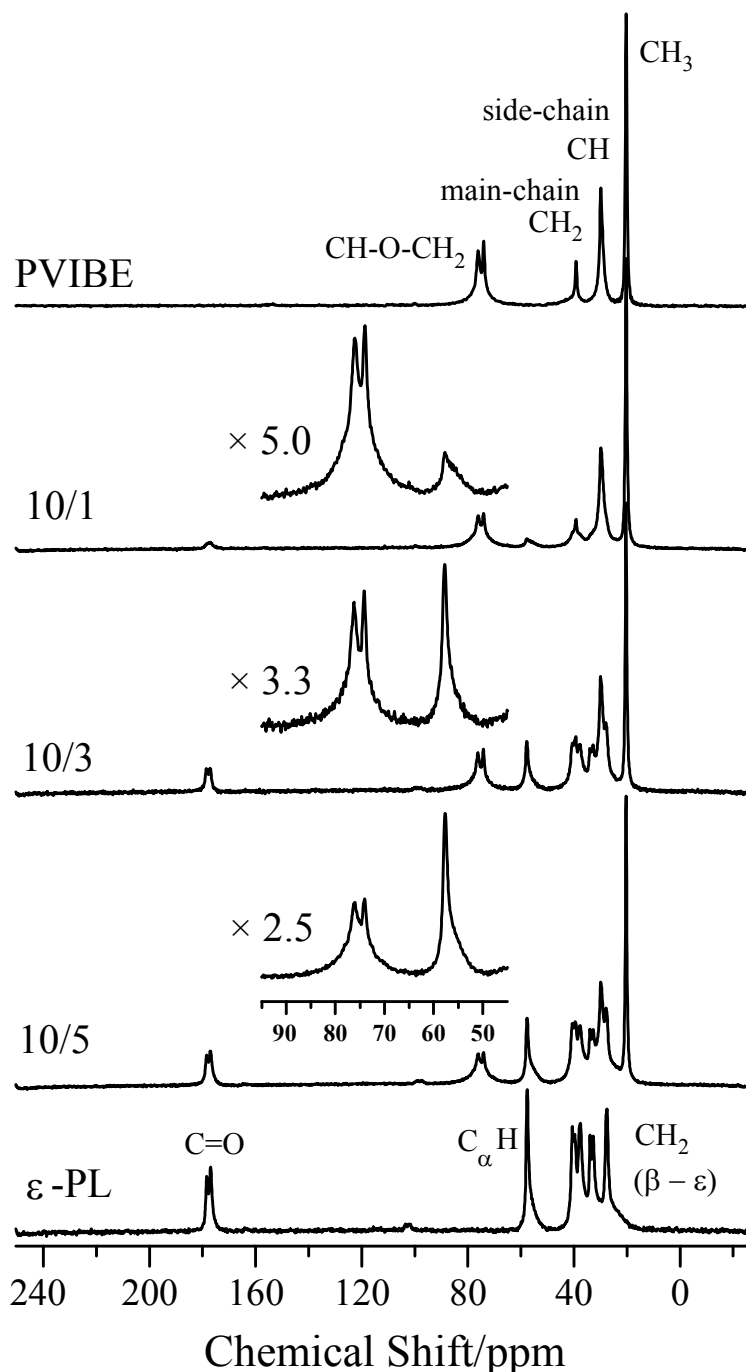


Figure 1. Observed  $^{13}\text{C}$  CPMAS NMR spectra of pure PVIBE, pure  $\epsilon$ -PL, and the PVIBE/ $\epsilon$ -PL blends at weight ratios of 10/1, 10/3, and 10/5. Expanded spectra at the aliphatic regions from 45 to 95 ppm for the blends are also shown.

example, the PVIBE cast from a chloroform solution shows a broad-line  $^{13}\text{C}$  peak of  $\text{CHOCH}_2$  at 75 ppm: similar spectrum can be seen in Figure 2(d). On the other hands, for PVIBE cast from a chloroform solution consisted with methanol, a doublet  $^{13}\text{C}$  peak of  $\text{CHOCH}_2$  appears at 76 and 74 ppm, that are attributed to the crystalline phase, on the broad-line peak as shown in Figure 1. Thus, the chloroform/methanol solvent ratio is carefully controlled.

The chemical shifts of the peaks assigned to PVIBE are not changed in the PVIBE/ $\epsilon$ -PL blends, and similar criterion holds on those of  $\epsilon$ -PL. This indicates that there is no interaction, which influences the  $^{13}\text{C}$  NMR spectra, between PVIBE and  $\epsilon$ -PL in the blends. However, Figure 1 shows that the peak shape of  $\text{C}_\alpha\text{H}$  signal of  $\epsilon$ -PL observed at 57.8 ppm is largely affected by blending of PVIBE, especially in the PVIBE/ $\epsilon$ -PL=10/1 blend. The sharp peak on a broad line disappears mostly. Furthermore, for the PVIBE/ $\epsilon$ -PL=10/5 blend, the doublet peaks at 76 and 74 ppm of PVIBE become small as compared to those of pure PVIBE or 10/1 and 10/3 blends. Of course, while the signal intensity is largely distorted via the CP depending on the difference of molecular motion, these observations indicate that the crystallinity of both PVIBE and  $\epsilon$ -PL is affected by blending each other. This implies that the miscibility will be influenced by the change of crystallinity or mixing ratio.

To investigate the crystallinity, we obtained the  $^{13}\text{C}$  CPMAS NMR spectra separated into contributions arising from the crystalline (CR) and non-crystalline (NC) phases by basing on the differences in the intrinsic  $^1\text{H}$  spin-lattice relaxation time in the rotating frame ( $T_{1\rho}^{\text{H}}$ ), that characterize the CR and NC phases [7, 8]. Figure 2 shows the expanded and separated spectra for the PVIBE/ $\epsilon$ -PL=10/5 blend; (a – d) are  $\text{CHOCH}_2$  regions for PVIBE and (e – h) are  $\text{C}_\alpha\text{H}$  regions for  $\epsilon$ -PL. Figures 2 (a, e) and (b, f) correspond, respectively, to 1  $\mu\text{s}$  and 3 ms  $^1\text{H}$  spin-locking times prior to the 800  $\mu\text{s}$  CP time. The relatively narrower peaks are emphasized in Figure 2 (b, f). This indicates that the intensity contribution from the CR phase is much greater in Figure 2 (b, f), because the  $T_{1\rho}^{\text{H}}$  is much shorter in the NC phase than in the CR phase. The CR and NC spectra of  $\epsilon$ -PL are also observed previously by basing on the differences in the  $^{13}\text{C}$  spin-lattice relaxation time in the laboratory frame ( $T_1^{\text{C}}$ ) [2]. Furthermore, a spectrum obtained for PVIBE cast from chloroform was attributable to the NC phases. Thus, we have known the signal shape of the NC region. Figures 2 (c, g) and (d, h) are linear combinations of Figures 2 (a, e) and (b, f) where we have attempted to null the NC and CR signal contributions, respectively. The linear combinations for PVIBE and  $\epsilon$ -PL are achieved individually, because the  $T_{1\rho}^{\text{H}}$  value characterized the NC phase for PVIBE is extremely faster than that for  $\epsilon$ -PL, so that the degree of decrease of the peak intensity after 3 ms  $^1\text{H}$  spin locking for PVIBE is different from that for  $\epsilon$ -PL. The spectra of Figures 2 (c) and (d) produce the whole spectrum of Figure 2 (a). Similarly, the spectra of Figure 2 (e) are reproduced by those of Figures 2 (g) and (h).

The crystallinity is estimated from the relative contribution of the CR component of the whole CPMAS  $^{13}\text{C}$  spectrum after a CP time of 800  $\mu\text{s}$ . The relative CR contribution is obtained from the integral of Figure 2 (c, g). The relative NC contribution is similarly given. Since both integrals are distorted during the 800  $\mu\text{s}$  CP time, corrections for a different CP efficiency are performed. The obtained crystallinity for pure PVIBE is 20 % and for pure  $\epsilon$ -PL is 54 %. These values have an experimental uncertainty within 5 %. The value of 54 % for pure  $\epsilon$ -PL is relatively smaller than the

previous value of 63 % obtained by Maeda, *et al.* [2]. This is due to a difference between the current and previous sample preparations as mentioned above, and may be also a difference in the estimation method. The previous method is based on the difference in  $T_1^C$ . For the method based on  $T_1^C$  difference, the CR region will be included some amounts of an interface that has the similar molecular motion as that of the CR. While for the current method, the spectrum of the NC region will contain the interface region, because the narrower peak attributed to the CR phase is induced by the higher order and the lower molecular motion.

The crystallinity of PVIBE in the PVIBE/ $\epsilon$ -PL blends was estimated as about 10-15 %, except for that in the PVIBE/ $\epsilon$ -PL=10/5 blend. The degree of PVIBE crystalline phase in the PVIBE/ $\epsilon$ -PL=10/5 blend is approximately 5 %. After blending with  $\epsilon$ -PL, the crystallinity of PVIBE become roughly half as compared to that of pure PVIBE. On the other hands, the crystallinity of  $\epsilon$ -PL in the PVIBE/ $\epsilon$ -PL blends were not so much influenced by blending with PVIBE, the values are 50-65 %, except for the PVIBE/ $\epsilon$ -PL=10/1 blend: the degree is approximately 30 %. These observations suggest that the growth of crystalline phase of PVIBE is largely affected by blending with  $\epsilon$ -PL, while the crystallization of  $\epsilon$ -PL is not significantly hindered by the blending with PVIBE. However, for the PVIBE/ $\epsilon$ -PL=10/1 blend, the crystallization of  $\epsilon$ -PL is impeded by much amounts of PVIBE. The miscibility will, thus, depend on the compositions of  $\epsilon$ -PL in the blend.

**Miscibility.** To study the miscibility, we measured the  $^1\text{H}$  spin-lattice relaxation decays in the laboratory frames ( $T_1^{\text{H}}$ ) via well-resolved  $^{13}\text{C}$  NMR. A CP from  $^1\text{H}$  to  $^{13}\text{C}$  enables us to detect the  $^1\text{H}$  decays for both PVIBE and  $\epsilon$ -PL independently. For a homogeneous blend, we observe that each  $^1\text{H}$  magnetization decays with the

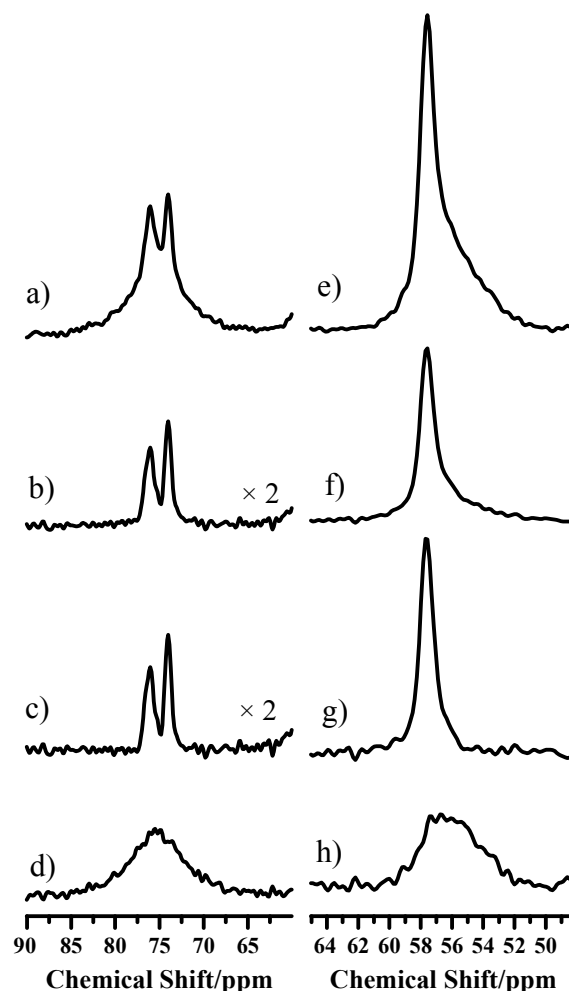


Figure 2. Expanded and separated  $^{13}\text{C}$  CPMAS NMR spectra for the PVIBE/ $\epsilon$ -PL=10/5 blend based on  $T_{1\rho}^{\text{H}}$  difference into the NC and the CR phases: the  $\text{CHOCH}_2$  peaks of PVIBE are on the left and  $\text{C}_\alpha\text{H}$  peak of  $\epsilon$ -PL on the right. Spectra (a, e) and (b, f) are the CP contact time of  $1\mu\text{s}$  and  $3\text{ms}$ , respectively. Spectra (c, g) and (d, h) are the CR phase and the NC phase, respectively.

same  $T_1^H$  value, because the fast  $^1\text{H}$  spin diffusion averages spin temperature of almost all the protons in a polymer blend. For a heterogeneous blend, we observe the independent  $T_1^H$  values from both components, that the  $T_1^H$  values are the same as the intrinsic  $T_1^H$  values for a pure component. In these cases, the  $^1\text{H}$  relaxation shows a single exponential decay. When the blend is partially miscible, the  $T_1^H$  values do not agree with each other but the  $T_1^H$  relaxation curves become characteristic non-exponential decays with an insufficient  $^1\text{H}$  spin-diffusion rate [9]. By estimating the  $^1\text{H}$  spin-diffusion rate  $k_d$ , we can obtain information of closeness using the relation of  $\langle r^2 \rangle = 6Dt_d$ ;  $r$  is the maximum diffusive path-length,  $D$  is the  $^1\text{H}$  spin-diffusion coefficient, and  $t_d$  is a diffusion time and

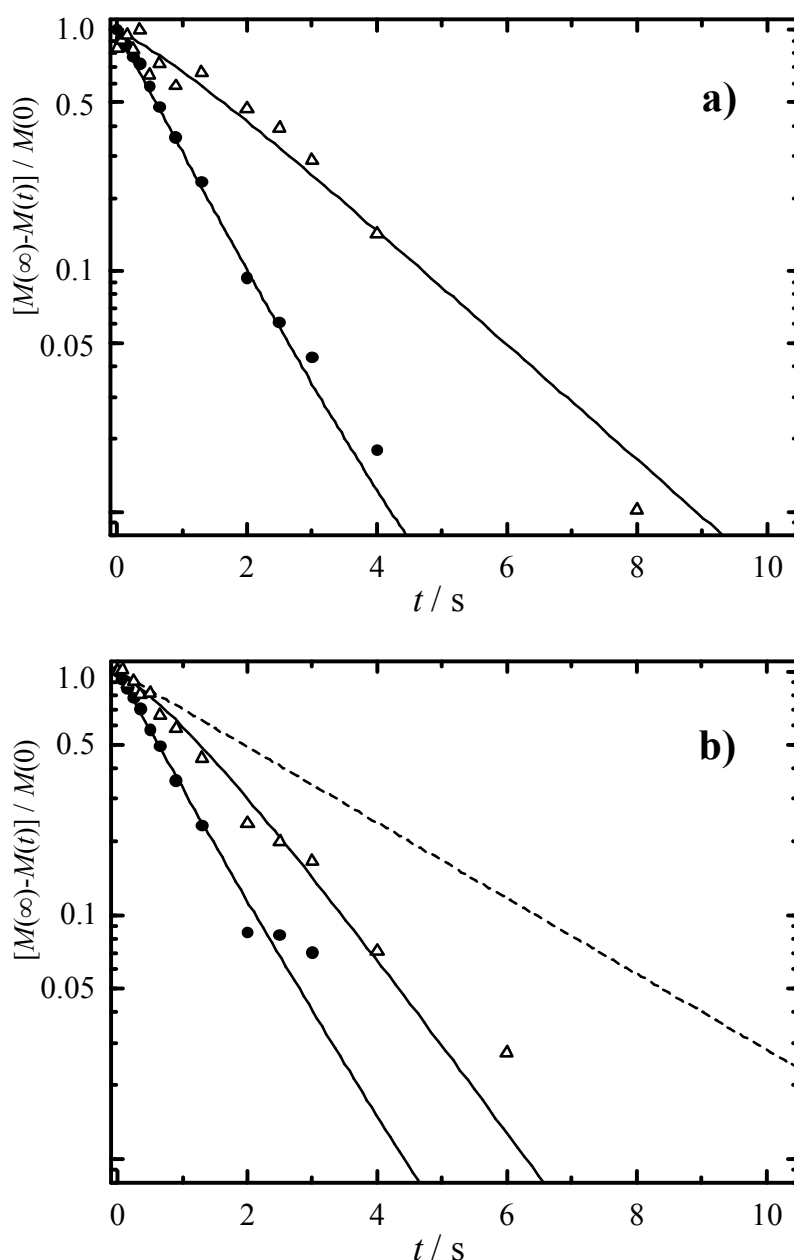


Figure 3. Observed  $T_1^H$  relaxation curves for both CR phases (a) and for both NC phases (b) of PVIBE (●) and  $\epsilon$ -PL ( $\triangle$ ). Each solid line represents the calculated curve from the eq. (1). The broken line is the  $T_1^H$  relaxation line of pure  $\epsilon$ -PL: the  $T_1^H$  value is 2.8 s.

equal to  $1/k_d$  [9, 10]. Therefore, the observation of both  $^1\text{H}$  magnetization decays ( $T_1^{\text{H}}$  relaxation curves) gives useful information on miscibility qualitatively and quantitatively. In the current case, furthermore, information about distances between the CR phases of PVIBE and  $\varepsilon$ -PL, and between the NC phases of PVIBE and  $\varepsilon$ -PL may be obtained from the  $T_1^{\text{H}}$  decays.

Figure 3 shows the observed  $T_1^{\text{H}}$  relaxation curves for PVIBE ( $\bullet$ ) and  $\varepsilon$ -PL ( $\triangle$ ) in the PVIBE/ $\varepsilon$ -PL=10/1 blend; (a) for both CR phases of PVIBE and  $\varepsilon$ -PL, (b) for both NC phases. In Figure 3 (b), the  $T_1^{\text{H}}$  decay of pure  $\varepsilon$ -PL is also depicted as a broken line. For pure PVIBE and pure  $\varepsilon$ -PL, the respective obtained  $T_1^{\text{H}}$  values from the CR and the NC phases were the same each other. It is clear that the observed  $T_1^{\text{H}}$  relaxation decays on a semi-log plot are not simple-straight lines, especially the initial several data points of  $\varepsilon$ -PL ( $\triangle$ ) show a curved line. Furthermore, the magnetization decay of  $\varepsilon$ -PL is different from that of pure one. Similar  $T_1^{\text{H}}$  decay curves are observed for the other blends. These observations indicate that the insufficient  $^1\text{H}$  spin diffusion occurs between PVIBE and  $\varepsilon$ -PL during the measuring period, and the blends are immiscible on a scale of 20-50 nm but partially miscible on a scale of 100 nm. Furthermore, it is worth noting that the decay curves in Figure 3 (a) is different from that in Figure 3 (b). This shows that the domain size of between the CR phases is different from that between the NC phases: similar results are observed for the PVIBE/ $\varepsilon$ -PL=10/3 blend, however, such a difference in  $T_1^{\text{H}}$  curves were not detected in the other blends.

To estimate the contribution of the  $^1\text{H}$  spin diffusion between PVIBE and  $\varepsilon$ -PL, we simulated the observed  $T_1^{\text{H}}$  relaxation curves using the two-spin model with a  $^1\text{H}$  spin-diffusion rate ( $k_d$ ). The  $^1\text{H}$  magnetization decay curves  $M_i(t)$  can be given as [9]

$$M_A(t) = a_+ e^{r_+ t} + a_- e^{r_- t} \quad (1)$$

$$M_B(t) = b_+ e^{r_+ t} + b_- e^{r_- t}$$

with

$$a_{\pm} = \frac{1}{2} \left\{ 1 \pm R^{-1} (K_B + k_d - K_A) \right\}, \quad b_{\pm} = \frac{1}{2} \left\{ 1 \pm R^{-1} (K_A + k_d - K_B) \right\},$$

$$r_{\pm} = \frac{1}{2} \left\{ -(K_A + K_B + k_d) \pm R \right\}, \quad R = +\sqrt{[(K_A - K_B) + (f_B - f_A)k_d]^2 + 4f_A f_B k_d^2}$$

where A and B represent PVIBE and  $\varepsilon$ -PL, respectively.  $K$  and  $f$  denote the intrinsic initial relaxation rate ( $= 1/T_1^{\text{H}}$ ) and  $^1\text{H}$  molar fraction, respectively. The initial magnetizations ratio  $M_A^0 : M_B^0$  is assumed to be  $f_A : f_B$ . The calculated ‘best-fit’ curves are depicted as solid lines in Figure 3. The calculated curves are in good agreement with the observed data points. The obtained values are  $K_A = 1.17 \text{ s}^{-1}$ ,  $K_B = 0.33 \text{ s}^{-1}$ , and  $k_d = 0.25 \text{ s}^{-1}$  for (a), and for (b),  $K_A = 1.12 \text{ s}^{-1}$ ,  $K_B = 0.39 \text{ s}^{-1}$ , and  $k_d = 0.57 \text{ s}^{-1}$ . For the other blends, the estimated  $k_d$  values are 0.1–0.2  $\text{s}^{-1}$ , except for the CR phases in the PVIBE/ $\varepsilon$ -PL=10/3 blend: the  $k_d$  is 0.34  $\text{s}^{-1}$ . The standard deviation is within 5%.

For the PVIBE/ $\varepsilon$ -PL=10/1 blend, the  $^1\text{H}$  spin-diffusion rate between the NC phases of PVIBE and  $\varepsilon$ -PL is more than twice as fast as that between the CR phases. It is noted again that the crystallinity of  $\varepsilon$ -PL in the PVIBE/ $\varepsilon$ -PL=10/1 blend is low and roughly half as compared to the other blends. These results suggest that the NC phase of PVIBE is in close proximity to that of  $\varepsilon$ -PL, and then the

crystallization of  $\epsilon$ -PL is deeply hindered by the NC phase of PVIBE. The domain size is roughly estimated to 100 nm with the typical  $^1\text{H}$  spin-diffusion coefficient in a polymer of ca.  $10^3 \text{ nm}^2\text{s}^{-1}$ . On the contrary to the PVIBE/ $\epsilon$ -PL=10/1 blend, for the PVIBE/ $\epsilon$ -PL=10/5 blend, the crystallinity of PVIBE is low and roughly half as compared to the other blends. In this case, the  $k_d$  values are  $0.10 \text{ s}^{-1}$  for the CR phases and  $0.15 \text{ s}^{-1}$  for the NC phases. The deduced domain size is over 200 nm. The obtained  $k_d$  value of  $0.1 \text{ s}^{-1}$  is close to a lower limitation to detect the contribution of a  $^1\text{H}$  spin diffusion; the lower limit in this case is around  $0.05 \text{ s}^{-1}$ . This observation indicates that the PVIBE/ $\epsilon$ -PL=10/5 blend is immiscible. The relatively large amount of  $\epsilon$ -PL can form its own CR/NC domain independently even in the PVIBE/ $\epsilon$ -PL blends.

For the PVIBE/ $\epsilon$ -PL=10/3 blend, interestingly, the  $^1\text{H}$  spin-diffusion rate between the CR phases of PVIBE and  $\epsilon$ -PL is obtained as a relatively large value of  $0.34 \text{ s}^{-1}$ . This value gives a domain size of 130 nm. For the other blends, the CR domain size between PVIBE and  $\epsilon$ -PL is approximately 180 – 250 nm [11]. It is shown that the CR regions of the PVIBE/ $\epsilon$ -PL=10/3 blend are an coexistent state of the two CR phases in a ca. 130 nm domain. The results suggest that the PVIBE/ $\epsilon$ -PL=10/3 weight-mixing ratio may be close to a critical value for the CR regions to be miscible in the PVIBE/ $\epsilon$ -PL blends.

### Conclusions

We showed that the miscibility of the NC regions is largely related to the crystallinity but that of the CR regions has been little related. It is found that the CR phase of PVIBE is in close proximity to that of  $\epsilon$ -PL only in the PVIBE/ $\epsilon$ -PL=10/3 blend. The analysis of the  $^1\text{H}$  spin-lattice relaxation decay curves enables us to obtain useful information for a location of the NC and CR phases.

### References

- 1) I.-L. Shih, M.-H. Shen, Y.-T. Van, *Bioresource Technology*, 2005 in press. (available online 18 October 2004)
- 2) S. Maeda, K. Kunimoto, C. Sasaki, A. Kuwae, K. Hanai, *J. Mol. Struct.*, **655**, 149 (2003).
- 3) S. Maeda, T. Mori, C. Sasaki, K. Kunimoto, A. Kuwae, K. Hanai, *Polym. Bull.*, **53**, 259 (2005).
- 4) A.E. Bennet, C.M. Rienstra, M. Auger, K.V. Lakshmi, R.G. Griffin, *J. Chem. Phys.*, **103**, 6951 (1995).
- 5) O.B. Peersen, X. Wu, I. Kustanovich, S.O. Smith, *J. Magn. Reson.*, **A104**, 334 (1993).
- 6) G. Metz, X. Wu, S.O. Smith, *J. Magn. Reson.*, **A110**, 219 (1994).
- 7) D.L. VanderHart, E. Pérez, *Macromolecules*, **19**, 1902 (1986).
- 8) D.L. VanderHart, A. Asano, J.W. Gilman, *Chem. Mater.*, **13**, 3781 (2001).
- 9) E.O. Stejskal, J. Schaefer, M.D. Sefcik, R.A. McKay, *Macromolecules*, **14**, 275 (1981).
- 10) A. Asano, K. Takegoshi : “*solid state NMR of polymers*”, Ed. I. Ando, T. Asakura, Elsevier, Amsterdam (1990), p.351.
- 11) For the PVIBE/ $\epsilon$ -PL=10/1 blend, the  $k_d$  of  $0.25 \text{ s}^{-1}$  is obtained for the CR phases. By using this value the domain size can be calculated to 155 nm. However, this value is probably largely affected by the  $^1\text{H}$  spin diffusion from the neighboring NC phase of PVIBE, too. Therefore, we eliminated this value from the estimation of the domain size of the CR regions.